



CrossMark
click for updates

Cite this: *RSC Adv.*, 2016, 6, 86373

Direct surface modification of poly(VDF-co-TrFE) films by surface-initiated ATRP without pretreatment†

Motoyasu Kobayashi,^{‡,ab} Yuji Higaki,^{abcd} Taichi Kimura,^c Frédéric Boschet,^e Atsushi Takahara^{*abcd} and Bruno Ameduri^e

The direct surface modification of poly(vinylidene fluoride-co-trifluoroethylene) (VDF-co-TrFE) copolymer films *via* surface-initiated atom transfer radical polymerization (ATRP) is presented. The surface-initiated ATRP of *tert*-butyl acrylate (tBA) and styrene was carried out on poly(VDF-co-TrFE) films containing 75 mol% VDF at 383 K. Such a reaction was monitored by ¹H and ¹⁹F NMR, attenuated total reflectance Fourier transform infrared (ATR-FTIR) spectroscopy, X-ray photoelectron spectroscopy (XPS), and by water contact angle measurements. First, the ¹⁹F NMR spectra of poly(VDF-co-TrFE)-*g*-poly(tBA) graft copolymers revealed a reduction in the signal intensity at –123 ppm compared with that of the poly(VDF-co-TrFE) copolymer, indicating that the polymerization of tBA occurred exclusively by fluorine abstraction from the TrFE units. ATR-FTIR spectra of the resulting poly(VDF-co-TrFE)-*g*-poly(tBA) and poly(VDF-co-TrFE)-*g*-polystyrene (PS) films evidenced the characteristic absorption frequencies assigned to carbonyl and aromatic C–H stretching. The atomic ratio on the surface of polymer-grafted poly(VDF-co-TrFE) film observed by XPS well agreed with theoretical value of poly(tBA) and PS homopolymers. These results indicated that poly(tBA) and PS were successfully grafted onto the poly(VDF-co-TrFE) film surfaces forming grafting layers, the thickness of which was over 10 nm. The poly(VDF-co-TrFE)-*g*-poly(tBA) film was subsequently treated with *p*-toluenesulfonic acid and sodium hydrogen carbonate to modify the grafted chains into poly(acrylic acid sodium salt). Surface-grafted polystyrene was also converted to poly(styrene sulfonic acid sodium salt) by treatment with sulfonic acid. Each reaction step was characterized by ATR-IR and XPS. The static water contact angle of poly(VDF-co-TrFE) copolymer was remarkably reduced from 91 to 15° by hydrolysis of the tBA chains, sulfonation of the styrene chains and their neutralization. A hydrophilic surface was successfully achieved on the poly(VDF-co-TrFE) film by direct surface-initiated polymerization from the outermost surface of the TrFE unit without any change in the bulk physical properties.

Received 19th July 2016
Accepted 4th September 2016

DOI: 10.1039/c6ra18397b

www.rsc.org/advances

Introduction

Fluorinated polymers are valuable materials with various remarkable properties, which are not exhibited in other organic

polymers.^{1–7} Among various synthetic pathways for the surface modification of fluorinated polymers, the direct “grafting-from” procedure from fluorinated polymer artifacts, which include films, fibers and membranes, seems the most appropriate pathway.⁸ Various studies regarding polymer-grafting, which is achieved by the polymerization of various monomers, such as acrylate or styrene derivatives, onto activated fluorinated polymers, such as poly(tetrafluoroethylene) (PTFE),^{9,10} poly(chlorotrifluoroethylene) (PCTFE),¹¹ and poly(vinylidene fluoride) (PVDF),^{2–4} or copolymers, such as poly(ethylene-co-tetrafluoroethylene) (ETFE),¹² poly(TFE-co-hexafluoropropylene) (FEP),¹³ poly(TFE-co-alkoxyethylene) (PFA),¹⁴ poly(VDF-co-hexafluoropropylene),¹⁵ poly(VDF-co-TFE),¹⁶ and poly(VDF-co-trifluoroethylene) (VDF-co-TrFE)³ copolymers, have been reported for a wide variety of applications such as fuel cell membranes and corrosion protection coatings. Because of the chemical stability of fluorinated polymers, the pretreatment of the fluorinated polymers is necessary for the “grafting-from” procedure. The activation has been accomplished by ozonization,^{3,5,17} by

^aJapan Science Technology Agency, ERATO, Takahara Soft Interfaces Project, 744 Motoooka, Nishi-ku, Fukuoka 819-0395, Japan

^bInstitute for Materials Chemistry and Engineering, Kyushu University, 744 Motoooka, Nishi-ku, Fukuoka 819-0395, Japan. E-mail: takahara@cstf.kyushu-u.ac.jp

^cGraduate School of Engineering, Kyushu University, 744 Motoooka, Nishi-ku, Fukuoka 819-0395, Japan

^dInternational Institute for Carbon-Neutral Energy Research (WPI-I2CNER), 744 Motoooka, Nishi-ku, Fukuoka 819-0395, Japan

^eIngénierie et Architectures Macromoléculaires, Institut Charles Gerhardt-UMR (CNRS) 5253, Ecole Nationale Supérieure de Chimie de Montpellier, 8 Rue de l'Ecole Normale, F-34296 Montpellier Cedex, France

† Electronic supplementary information (ESI) available. See DOI: 10.1039/c6ra18397b

‡ Present address: School of Advanced Engineering, Kogakuin University, 2665-1 Nakano-cho, Hachioji, Tokyo 192-0015, Japan.

high energy technologies such as gamma rays,¹⁸ swift heavy ions,^{19,20} electron beam,^{21–23} or plasma.²⁴ Conventional free radical polymerization strategy was also applied to surface modification by means of a fluorinated copolymer bearing a peroxy carbonate radical initiator.²⁵

The “grafting-from” procedure based on controlled radical polymerization (CRP) techniques has attracted considerable interest due to the possibility to control the macromolecular architecture. The polymer grafting on PVDF-based macroinitiators through nitroxide-mediated living free radical polymerization (NMP),²⁶ atom transfer radical polymerization (ATRP)^{27–34} and reversible addition–fragmentation chain transfer (RAFT)^{35–37} has been reported, as shown in Table 1. ATRP is regarded as the most pertinent strategy for the fluorinated copolymers because the technique utilizes a reversible cleavable of C–X (where X represents a halogen) bond in the backbone, and is widely used as an efficient polymerization for well-defined graft copolymers preparation. Fluorinated copolymers having C–Cl and C–Br groups at the backbone have been used to initiate ATRP by the reversible activation of the C–X bonds,^{38–41} whereas C–F bond is too stable (*ca.* 486 kJ mol^{−1}) to initiate the polymerization.³⁰ Mayes *et al.*⁴² reported surprising direct preparation of the graft copolymer of methacrylates from PVDF *via* ATRP using secondary fluorine as the initiator.

Characterization of SEC and ¹H NMR of graft copolymer obtained by solution method, and XPS study of a copolymer film prepared by grafting from PVDF membrane revealed the graft polymerization was directly initiated from PVDF.

Until now, huge number of ATRP with PVDF macroinitiator has been further reported.^{11,27–34,38–45} Table 1 lists research works on “surface-grafting” from outermost surface of fluoropolymer film or membranes by radical method, and related studies on the grafting from macroinitiator in solution. Nandi *et al.*³¹ have reported that the polymerization of *N,N*-dimethylaminoethyl methacrylate (DMAEMA) was initiated from head-to-head defects of the PVDF macroinitiator to give PVDF-*g*-poly(DMAEMA) graft copolymers with increasing graft density for longer polymerization times. On the other hand, the direct surface-initiated ATRP from the polymer articles including films, fibers, and porous membrane has been demonstrated not only for PVDF^{29–31,42,43} but also for polyethylene,^{11,46} polyester⁴⁷ and polyolefin articles.⁴⁸ Takahara *et al.*⁴⁹ reported the direct surface-initiated ATRP of *tert*-butyl acrylate (*t*BA) from poly(VDF-*co*-TrFE) films. Sundholm's group⁵⁰ performed the synthesis of PVDF-*g*-poly(vinyl benzyl chloride) (PVBC) graft copolymers by irradiation of PVDF by electron beam followed by grafting vinyl benzyl chloride (VBC). In a subsequent step, these PVDF-*g*-PVBC graft copolymers acted as suitable

Table 1 Overview of the synthesis of fluorinated graft copolymers achieved by radical method

Method ^a	Initiator or chain transfer ^b	Structure of F-graft ^c	Ref.
NMP	PVDF bearing TEMPO	PVDF- <i>g</i> -PSSA	26
RAFT	PVDF bearing dithioester group	PVDF- <i>g</i> -PPEOMA	35
		PVDF- <i>g</i> -PAA	36
	PVDF bearing azo group	PVDF- <i>g</i> -PPEOMA	37
		PVDF- <i>g</i> -PMMA	37
ATRP	PVDF	PVDF- <i>g</i> -PSSA	29, 42 and 43
		PVDF- <i>g</i> -poly(DMAEMA)	29 and 30
		PVDF- <i>g</i> -PSPMA	28
		PVDF- <i>g</i> -poly(BMA)	31
		PVDF- <i>g</i> -PMAA	42
		PVDF- <i>g</i> -PPEOMA	42
	PVDF- <i>g</i> -PVBC	PVDF- <i>g</i> -PVBC- <i>g</i> -PS	50
	P(VDF- <i>co</i> -CTFE)	P(VDF- <i>co</i> -CTFE)- <i>g</i> -poly(<i>t</i> BA)	11 and 51
		P(VDF- <i>co</i> -CTFE)- <i>g</i> -PS	11, 38 and 51
		P(VDF- <i>co</i> -CTFE)- <i>g</i> -PSSA	11, 33, 34, 38 and 44
		P(VDF- <i>co</i> -CTFE)- <i>g</i> -PPEOMA	11 and 52
	P(CTFE- <i>alt</i> -VE)	P(CTFE- <i>alt</i> -VE)- <i>g</i> -PSammonium	45
	P(VDF- <i>co</i> -TrFE)	Poly(VDF- <i>co</i> -TrFE)- <i>g</i> -poly(<i>t</i> BA)	49
		Poly(VDF- <i>co</i> -TrFE)- <i>g</i> -PAAsalt	49
	P(VDF- <i>co</i> -BDFO)	PVDF- <i>g</i> -PS	28
	P(VDF- <i>ter</i> -TrFE- <i>ter</i> -CTFE)	P(VDF- <i>ter</i> -TrFE- <i>ter</i> -CTFE)- <i>g</i> -PS	38 and 40
SET-LRP	P(VDF- <i>co</i> -CTFE)	P(VDF- <i>co</i> -CTFE)- <i>g</i> -PMMA	41
Uncontrolled	P(VDF- <i>co</i> -CTFE)- <i>g</i> -peroxy carbonate	P(VDF- <i>co</i> -CTFE)- <i>g</i> -PVDF	25
	PVDF ozonization	PVDF- <i>g</i> -PPEOMA	17
	PVDF bearing azo group	PVDF- <i>g</i> -PAA	36
Radio grafting	FP/irradiation	FP- <i>g</i> -PS, FP- <i>g</i> -PMMA	1

^a NMP, RAFT, ATRP, and SET-LRP stand for nitroxide-mediated polymerization, reversible addition fragmentation chain-transfer, atom transfer radical polymerization, single-electron transfer-living radical polymerization, respectively. ^b PVDF, TEMPO, PVBC, CTFE, VE, TrFE, BDFO, and FP stand for poly(vinylidene fluoride), 2,2,6,6-tetramethylpiperidinyl-1-oxy, poly(vinyl benzylchloride), chlorotrifluoroethylene, vinyl ether, trifluoroethylene, 8-bromo-1*H*,1*H*,2*H*-perfluorooct-1-ene, and fluoropolymers, respectively. ^c PSSA, PPEOMA, PAA, PMMA, DMAEMA, PSPMA, PS, *t*BA, PSammonium, BMA, and PMAA stand for styrene sulfonic acid, poly(oxyethylene) methacrylate, poly(acrylic acid), *N,N*-dimethylaminoethyl methacrylate, poly(3-sulfopropyl methacrylate), polystyrene, *tert*-butyl acrylate, poly(4-vinylbenzyltrimethylammonium salt), butyl methacrylate, and poly(methacrylic acid), respectively.

macroinitiators (via their chloromethyl side-groups) in the ATRP of styrene leading to controlled (PVDF-*g*-PVBC)-*g*-poly(styrene) (PS) graft copolymers. In another approach, Zhang and Russell⁵¹ prepared PVDF-*g*-PS and PVDF-*g*-poly(*t*BA) graft copolymers of molecular weights up to 250 000 g mol⁻¹ by ATRP initiated with a poly(VDF-*co*-CTFE) copolymer. Similarly, Koh *et al.*⁵² synthesized poly(VDF-*co*-CTFE)-*g*-poly(poly(oxyethyl methacrylate)) (PPOEMA), as an amphiphilic comb copolymer with hydrophobic poly(VDF-*co*-CTFE) backbone and hydrophilic PPOEMA side chains at 73/27 wt%. The microphase separation structure generated by poly(VDF-*co*-CTFE)-*g*-PPOEMA comb copolymer⁵² was useful to produce the homogeneous nanocomposite films containing the silver nanoparticles (average size was 4–8 nm) by the *in situ* reduction of trifluoromethanesulfonate precursor under UV irradiation. In the last decades, various types of hydrocarbon polymers, such as polybutadiene, polyisoprene, PMMA, PDMS, polyphosphazene, polysulfone, and poly(vinyl alcohol), were grafted from the perfluoroalkyl groups or the fluorinated (co)polymers.¹

Although various direct graft polymerization from fluoropolymers have been investigated as listed in Table 1, it was worth bringing spectroscopic proofs to elucidate ATRP initiation from CF₂ groups of PVDF or another site. Therefore, we started the project to study the evidence which is the cleavable bond involved in ATRP from the poly(VDF-*co*-TrFE) copolymer to initiate the graft polymerization. The detail spectroscopic analysis of ATRP with poly(VDF-*co*-TrFE) macroinitiator was also conducted by ¹⁹F and ¹H NMR to understand the polymerization mechanism. In addition, the graft polymerization strategy of poly(VDF-*co*-TrFE) copolymer was applied to the surface modification of fluoropolymer substrates by the surface-initiated ATRP of *t*BA and styrene directly from poly(VDF-*co*-TrFE) films. The change in surface wettability from hydrophobic to hydrophilic was also observed by the successive hydrolysis of butyl ester or sulfonation of phenyl groups.

Experimental

Materials

Vinylidene fluoride (VDF)–trifluoroethylene (TrFE) copolymer [poly(VDF-*co*-TrFE)] film (thickness = 80 μm) containing 75 mol% VDF units was provided by Daikin Industries. The number-average molecular weight (M_n) and molecular weight distribution of poly(VDF-*co*-TrFE) film were $M_n = 88\,700$ g mol⁻¹ and $M_w/M_n = 3.34$, respectively. The films were pressed between polished Si wafers (15 × 15 mm) under vacuum at 363 K under 40 MPa for 10 minutes to make the surface smooth for the characterization, and rinsed with hexane before use. Copper(i) chloride (CuCl, Wako Pure Chemicals) was purified by washing with acetic acid and ethanol, and was dried under vacuum. *tert*-Butyl acrylate (*t*BA), styrene and ethyl 2-chloropropionate (EC) were purchased from Tokyo Chemical Industry, and purified by distillation under reduced pressure over calcium hydride prior to use. Anisole and methanol were purchased from Wako Pure Chemicals and purified by distillation after reflux with metallic sodium for 4 hours. *N,N,N',N'',N'''*-Pentamethyldiethylenetriamine (PMDETA), and

4,4'-dimethyl-2,2'-bipyridyl (DMbpy) were purchased from Aldrich and used without further purification. Heptane, tetrahydrofuran (THF), sodium hydrogen carbonate (NaHCO₃), and *p*-toluene sulfonic acid monohydrate were purchased from Wako Chemicals and used as received. Sulfuric acid (Nacalai Tesque Inc.) and *N,N*-dimethylformamide (DMF, Kishida Chemical Co.) were used as received. Water for the contact angle measurement was purified with the NanoPure Water system (Millipore, Inc.). Deuterated acetone was purchased from Euriso-top (Grenoble, France) (purity > 99.8%). All other reagents and solvents were purchased from Wako Pure Chemicals and used as received.

Measurements

¹H NMR measurement was carried out on a Bruker AC 400 instrument, using deuterated acetone as the solvent and tetramethylsilane (TMS) as the references at 298 K. The experimental conditions for recording ¹H NMR spectra were as follow: flip angle 90°, acquisition time 4.5 s, pulse delay 2 s, and number of scans 128. ¹⁹F NMR spectroscopic measurement was carried out on a Bruker AC 400 instrument, using deuterated acetone as the solvent and CFCl₃ as the references at 298 K. The experimental conditions for recording ¹⁹F NMR spectra were as follows: flip angle 30°, acquisition time 0.7 s, pulse delay 2 s, number of scans 512, and a pulse width of 5 μs.

The M_n and the molecular weight distribution were determined by size exclusion chromatography (SEC) using a HLC-8220 system (TOSOH Co., Ltd.) equipped with three directly connected polystyrene gel columns of TSKgel SuperH6000, 4000 and 2500, and a refractive index (RI) detector. Tetrahydrofuran (THF) was used as the eluent at a flow rate of 0.6 mL min⁻¹ at 313 K. Calibration curves were prepared with a series of PS standards (3690 K, 672 K, 218.8 K, 52.2 K, 21.0 K, 4920, 1060 g mol⁻¹).

Attenuated total reflectance Fourier transformed infrared spectroscopy (ATR-FTIR) was carried out on a Spectrum One (Perkin Elmer Inc.). A ZnSe with a 45° angle crystal was used and all spectra were recorded at 1.0 cm⁻¹ resolution for 128 scans, and the empty ATR cell spectrum was used for background.

X-ray photoelectron spectroscopy (XPS) measurement was carried out using an XPS-APEX (Physical Electronics Inc.) at 1 × 10⁻⁹ Pa using a monochromatic Al K_α X-ray source operated at 200 W. XPS spectra were collected at takeoff angle of 45°, and a low-energy (25 eV) electron flood gun was used to minimize sample charging. The survey spectra (0–1000 eV) and high-resolution spectra (narrow scan) of the C_{1s} were acquired at an energy step of 1.0 and 0.1 eV, respectively. Sputter depth profiling using C₆₀⁺ ion source was recorded on a PHI Quantera SXM (ULVAC-PHI, Chigasaki, Japan) system using a micro-focused (100 μm, 24.8 W, 15 kV) Al X-ray beam (1486.6 eV) with a photoelectron take-off angle of 45°. Details are described in the ESI.†

Atomic force microscopy (AFM) observation was operated with the dynamic force mode at optimal force under ambient atmosphere at room temperature, using a 20 × 20 μm² PZT-

scanner with SPA 400 (SII NanoTechnology, Inc.). Rectangular shaped silicon cantilevers (tip radius: ~ 10 nm; SI-DF20; Seiko Instruments Inc.), with spring constant of 15 N m^{-1} and resonance frequency of 130 kHz, were used for imaging. The root mean square (rms) roughness (R_q) was calculated by the following equation;

$$R_q = \sqrt{\frac{1}{L} \int_0^L z(x)^2 dx} \quad (1)$$

where L and $z(x)$ are scanning distance and the height variation function of the surface along with the scanning direction (x), respectively.

The static contact angles against water ($2 \mu\text{L}$) were recorded with a drop-shaped analytical system DSA 10 (KRÜSS Co., Ltd.) equipped with a video camera. The average of five measurements were used as the data.

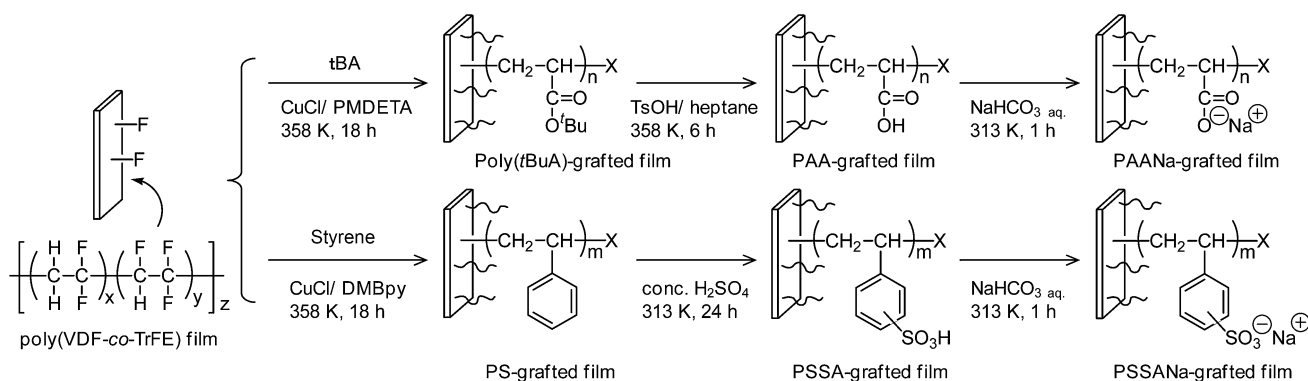
Solution polymerization of *t*BA from poly(VDF-*co*-TrFE) copolymer

Poly(VDF-*co*-TrFE) film (200 mg, VDF unit = 2.19 mmol, TrFE unit = 0.73 mmol), CuCl (8.0 mg, 0.081 mmol), PMDETA (22.2 mg, 0.128 mmol) were added in a glass vessel and dried by repeating a degas and argon purge. The *t*BA (5.00 mL, 34.0 mmol) and DMF (7.0 mL) were transferred into the glass vessel, and the poly(VDF-*co*-TrFE) film was dissolved in the solution.

Oxygen was removed by three freeze-thaw cycles. The reaction vessel was placed into an oil bath, and heated at 358 K for 80 min under argon atmosphere. After cooling to room temperature, the solution was diluted with small portion of methanol and poured into an excess volume of methanol aqueous solution (water/methanol = 4/1, vol/vol) to precipitate the resulting poly(VDF-*co*-TrFE)-*g*-poly(*t*BA) copolymer. The precipitated polymer was collected by vacuum filtration and dried under vacuum prior to the characterization.

Surface-initiated ATRP of *t*BA from poly(VDF-*co*-TrFE) film

A typical procedure of surface-initiated ATRP is described in Scheme 1. A poly(VDF-*co*-TrFE) film (200 mg), CuCl (8.0 mg, 0.081 mmol) and PMDETA (22.2 mg, 0.128 mmol) were added in a glass vessel and dried by repeating a degas and argon purge. The *t*BA (5.00 g, 34.0 mmol) and EC (10.9 mg, 0.08 mmol) were introduced into the glass vessel. Oxygen was removed by the freeze-thaw cycles. The reaction vessel was placed into an oil bath, and heated at 358 K for 18 h under argon atmosphere. The solution was diluted with a small portion of methanol and poured into an excess volume of methanol aqueous solution (water/methanol = 4/1, vol/vol) to precipitate unbound poly(*t*BA). The resulting poly(VDF-*co*-TrFE)-*g*-poly(*t*BA) film was washed by methanol with a Soxhlet apparatus for 24 h to remove the adsorbed free polymer, and dried under vacuum prior to the characterization. Surface-initiated ATRP of styrene was also



Scheme 1 Schematic diagram of the direct modification of the poly(VDF-*co*-TrFE) films by surface-initiated ATRP and the successive hydrolysis and sulfonation reactions.

Table 2 Direct surface-initiated ATRP of *tert*-butyl acrylate (*t*BA) and styrene (St) from poly(VDF-*co*-TrFE) film surface^a

Run	Amount of reagents (mmol)				Time h	$M_n \times 10^{-3}^b$	M_w/M_n^b
	CuCl	Ligand	EC	Monomer			
1	0.089	PMDETA: 0.131	0.080	<i>t</i> BA: 34.13	12	34.5	1.60
2	0.095	PMDETA: 0.131	0.080	<i>t</i> BA: 34.13	12	42.0	1.76
3	0.080	PMDETA: 0.128	0.070	<i>t</i> BA: 34.13	18	30.5	1.49
4	0.081	PMDETA: 0.128	0.070	<i>t</i> BA: 34.13	18	23.4	1.60
5	0.081	DMBpy: 0.162	0.070	St: 34.70	18	24.7	1.24

^a Polymerization were carried out under Ar at 358 K. ^b Determined by SEC using polystyrene standards. PMDETA, DMBpy, and EC stand for *N,N,N',N',N''*-pentamethyldiethylenetriamine, 4,4'-dimethyl-2,2'-bipyridyl, and ethyl 2-chloropropionate, respectively.

carried out under similar conditions in the presence of CuCl and DMbpy at 358 K, and the obtained poly(VDF-*co*-TrFE)-*g*-PS film was washed by toluene with a Soxhlet apparatus for 24 h. Table 2 lists the molecular weight and molecular weight distribution of the resulting unbound poly(*t*BA) and polystyrene.

Hydrolysis and neutralization of surface-tethered poly(*t*BA) chains

Heptane (20 mL), distilled water (0.5 mL) and *p*-toluenesulfonic acid monohydrate (0.2 g) were introduced in a glass vessel. Poly(VDF-*co*-TrFE)-*g*-poly(*t*BA) graft copolymer was introduced into the solution, and the glass vessel was placed into an oil bath, and heated at 358 K for 6 h. The film was washed with water, and dried under vacuum to yield the hydrolyzed poly(VDF-*co*-TrFE)-*g*-poly(acrylic acid) (PAA) film. The hydrolysis of *tert*-butyl ester was monitored by ATR-FTIR. The poly(VDF-*co*-TrFE)-*g*-PAA film was immersed into NaHCO₃ aqueous solution (0.01 g mL⁻¹). The solution was heated at 313 K for 60 min. The

film was washed with water, and dried under vacuum to yield the neutralized poly(VDF-*co*-TrFE)-*g*-poly(acrylic acid sodium salt) (PAANa) graft copolymer film.

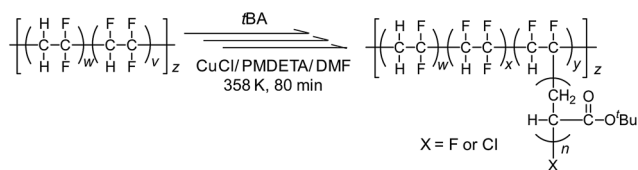
Sulfonation and neutralization of surface-tethered PS chains

Poly(VDF-*co*-TrFE)-*g*-PS film (Table 2, run 5) was introduced into a glass vessel and immersed into a concentrated sulfuric acid. The glass vessel was placed into an oil bath at 313 K for 24 h. The film was washed with water, and dried under vacuum to give the poly(VDF-*co*-TrFE)-*g*-poly(styrene sulfonic acid) (PSSA) film that was subsequently immersed into NaHCO₃ aqueous solution (0.01 g mL⁻¹) at 313 K for 60 min. The film was washed with water, and dried under vacuum to give the neutralized poly(VDF-*co*-TrFE)-*g*-poly(styrene sulfonic acid sodium salt) (PSSANa) film.

Results and discussion

Solution polymerization of *t*BA from poly(VDF-*co*-TrFE) copolymer

First of all, we carried out ATRP of *t*BA in DMF using poly(VDF-*co*-TrFE) copolymer (200 mg) as a macroinitiator in the presence of CuCl/PMDETA complex at 358 K for 80 min under argon atmosphere (Scheme 2) to give a poly(VDF-*co*-TrFE)-*g*-poly(*t*BA) graft copolymer with 210 mg yield. Therefore, the weight fraction of poly(*t*BA) was estimated to be 4.8 wt%. The resulting graft copolymer was characterized by ¹H and ¹⁹F NMR, as described in following section.



Scheme 2 Proposed mechanism of graft polymerization of *t*BA from poly(VDF-*co*-TrFE) via ATRP.

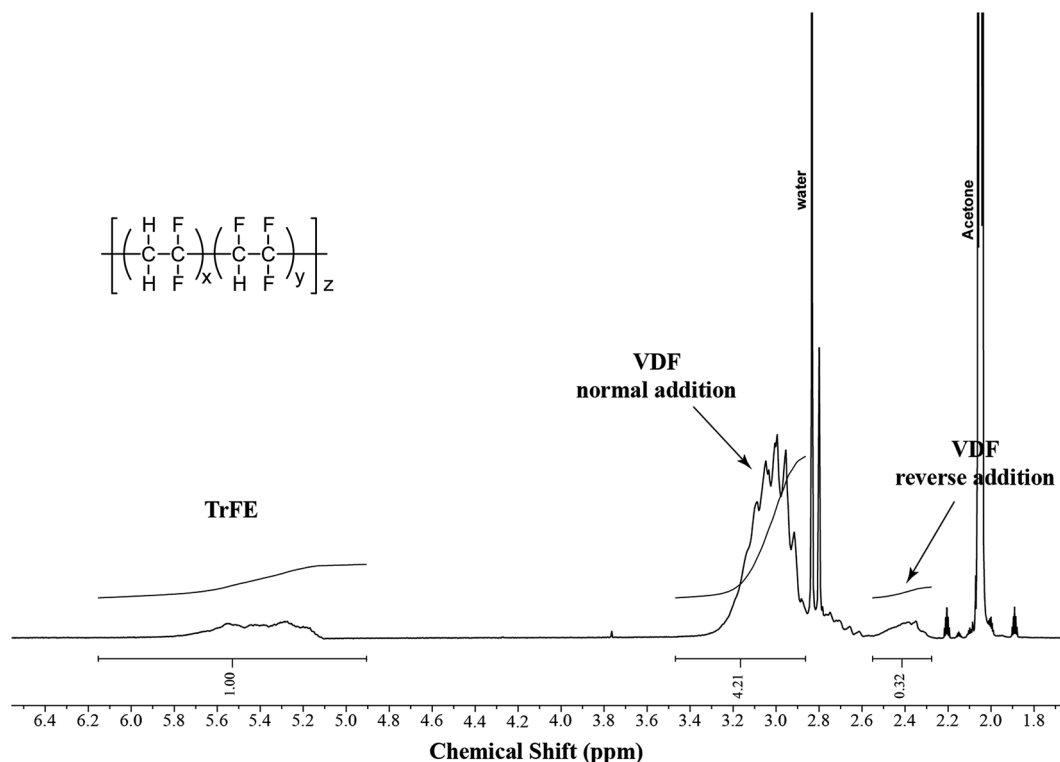


Fig. 1 ¹H NMR spectrum of the poly(VDF-*co*-TrFE) recorded in acetone-*d*₆.

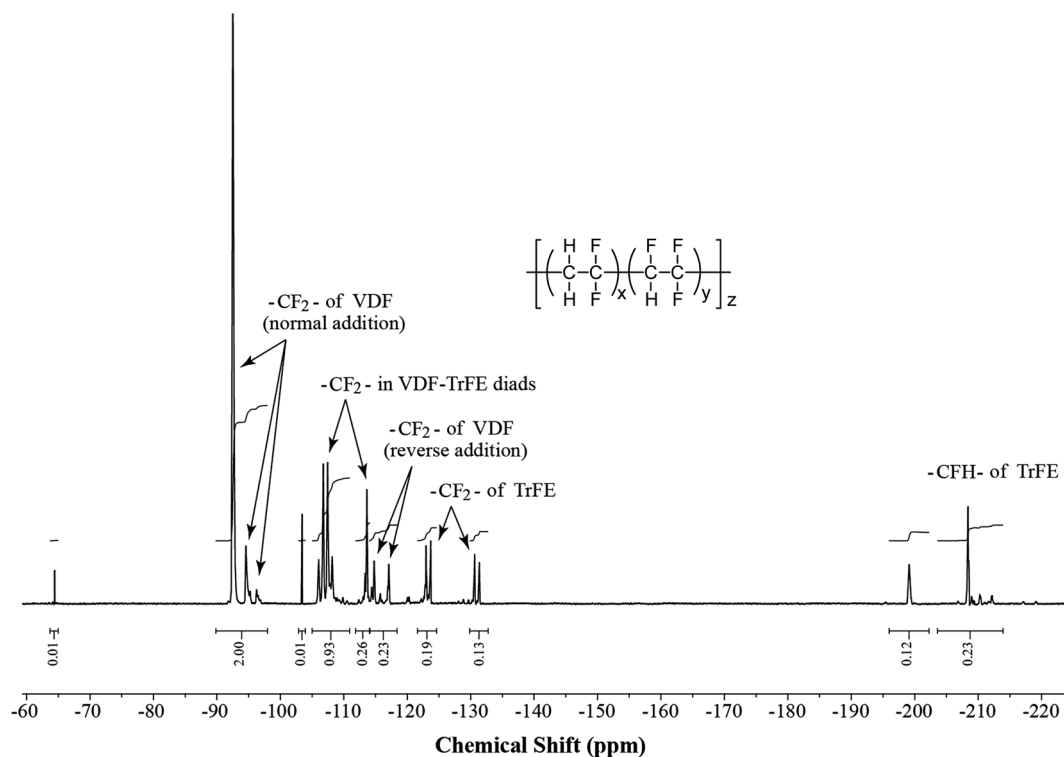


Fig. 2 ^{19}F NMR spectrum of the poly(VDF-co-TrFE) recorded in acetone- d_6 .

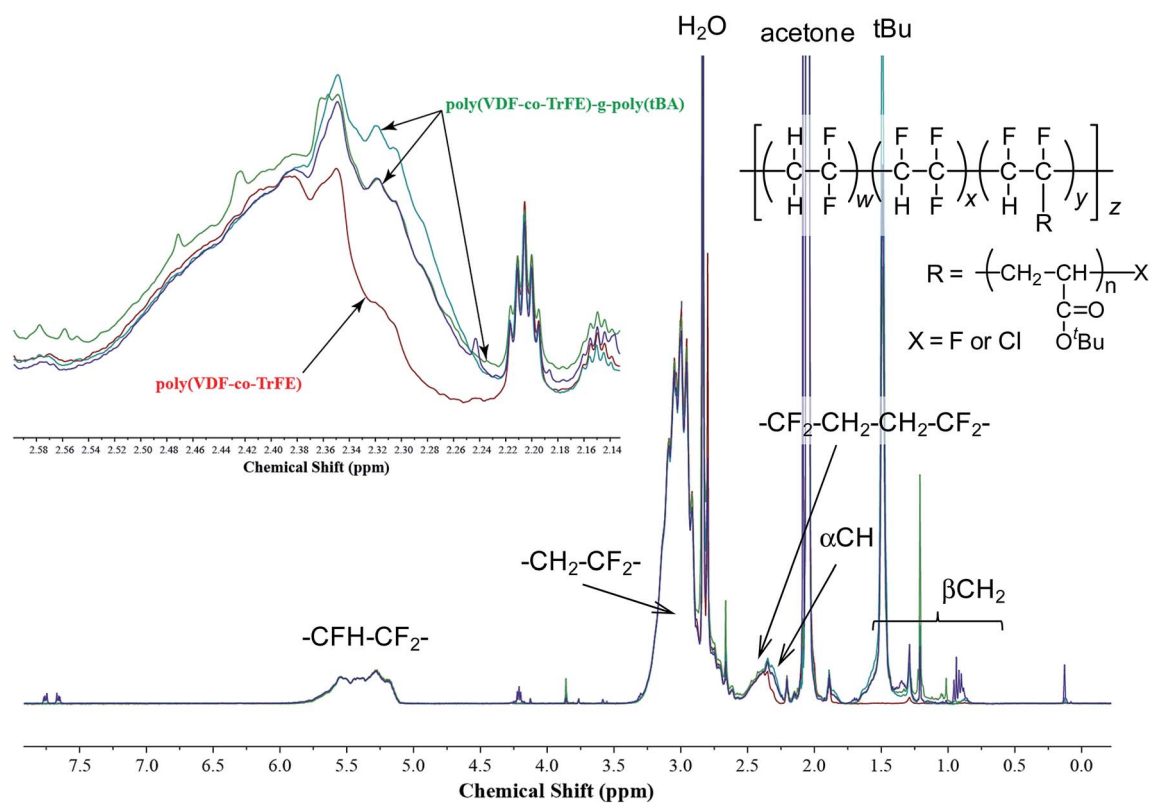


Fig. 3 ^1H NMR spectra of one poly(VDF-co-TrFE) (red line) and three poly(VDF-co-TrFE)-*g*-poly(tBA) (blue, green, purple lines). All the spectra were overlapped.

NMR analysis for the polymerization mechanism investigation

The ^1H NMR spectrum of poly(VDF-*co*-TrFE) copolymer shows signals for VDF assigned to the normal tail-to-tail additions and signals attributed to the reverse tail-to-tail additions at 2.8–3.3 ppm and 2.2–2.5 ppm, respectively (Fig. 1). The signals for –CHF– of TrFE units are located between 5.0 and 5.8 ppm.⁶ The integral of those signals indicates 71.4 mol% of VDF in the copolymer. In the case of Fig. 1, the content of VDF (C_{VDF}) was estimated as follows.

$$C_{\text{VDF}} = \frac{4.21 + 0.32/2}{4.21 + 0.32/2 + 1.0/1} \times 100 = 71.4\% \quad (2)$$

The ^{19}F NMR spectrum of poly(VDF-*co*-TrFE) displays signals for both VDF and TrFE. Signals for –CFH– of TrFE are found at –199 (TrFE–TrFE dyad) and –209 ppm (VDF–TrFE dyad), while –CF₂– signals for both VDF and TrFE are located between –92 and –132 ppm.⁶ Signals for –CF₂– of TrFE correspond to the two AB systems centered at –131 and –123.5 ppm. Inverse additions of VDF are located at –115 and –117 ppm. The signal centered at –107.6 ppm corresponds to a –CF₂– of VDF adjacent to a –CFH– of TrFE while the signal centered at –114 ppm was assigned to a –CF₂– of VDF adjacent to a –CF₂– of TrFE. Normal addition of VDF is located between –92 and –97 ppm (Fig. 2). Integrals of the signals indicate that the copolymer contain 70.4 mol% of VDF.

Fig. 3 exhibits a typical ^1H NMR spectrum of poly(VDF-*co*-TrFE)-*g*-poly(*t*BA) graft copolymer synthesized by solution polymerization of *t*BA with a poly(VDF-*co*-TrFE) macroinitiator in the presence of CuCl/PMDETA complexes in DMF. The ^1H NMR spectra do not show any changes for the signals at 3.0–3.3 ppm of VDF units and 5.0–5.8 ppm of TrFE units. A slight change is observed for the signal at 0.8–1.7 ppm and 2.3 ppm that were assigned to the presence of the methylene and methine protons of the *t*BA units, respectively, though as the change is small, only a few grafted chains are expected. A new singlet also appears at 1.4 ppm assigned the *tert*-butyl protons of *t*BA units. The weight fraction of grafted poly(*t*BA) chains was estimated to be around 3.6 wt%. It was assessed from the integral ratio of *t*Bu at 1.5 ppm and the sum of the integral of signals at 5.0–5.8 ppm and 3.0–3.3 ppm assigned to the CFH and CH₂ protons. Therefore, the grafting efficiency is not sufficient in this system and the polymerization initiates from a part of the main chain.

Fig. 4 exhibits a ^{19}F NMR spectrum of poly(VDF-*co*-TrFE)-*g*-poly(*t*BA). The superposition of the ^{19}F NMR spectra shows no changes in the intensities of the signals of the VDF units whereas all signals assigned to TrFE highlights some changes in chemical shifts and shape. These changes are attributed to the grafting reaction where the electron-donating *tert*-butyl ester group induces a high field chemical shift so that differences are noted at about –208.5 ppm and –199 ppm. The effect is also visible on the –CF₂– of TrFE adjacent to the graft (signals at

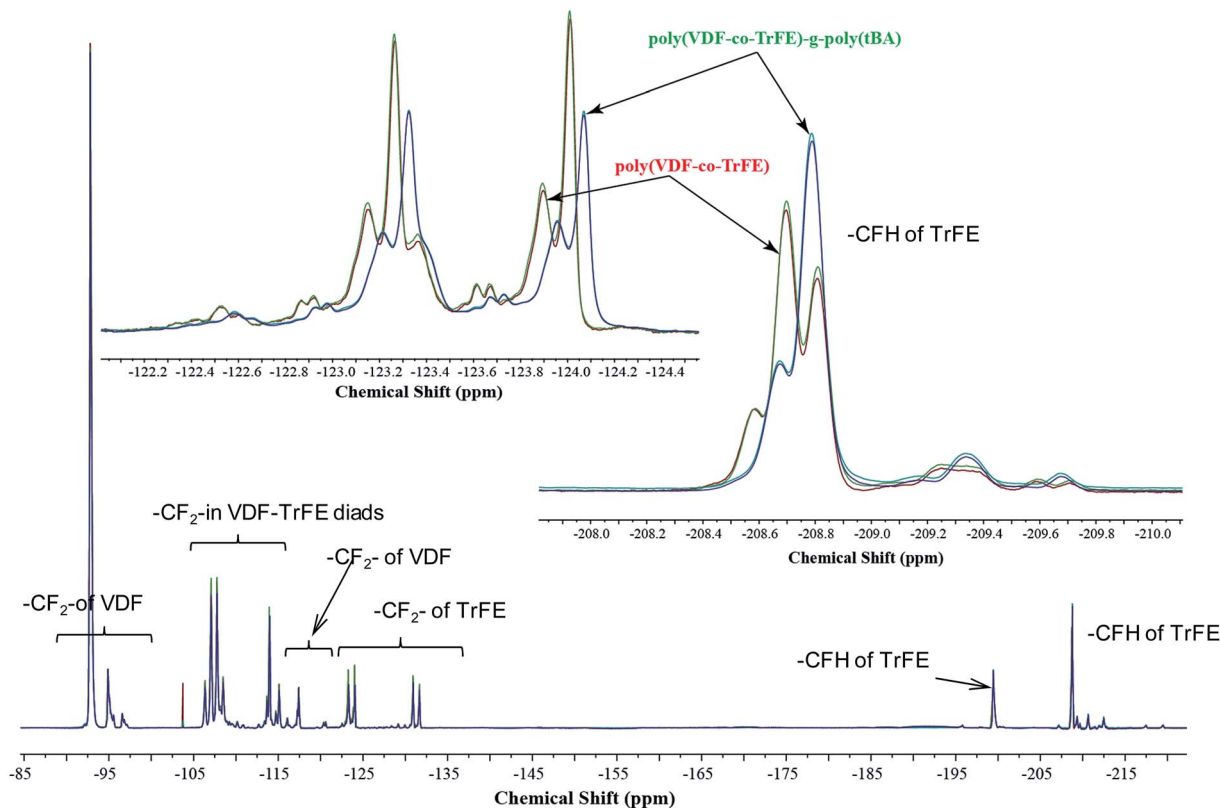


Fig. 4 ^{19}F NMR spectra of one poly(VDF-*co*-TrFE) (red line) and three poly(VDF-*co*-TrFE)-*g*-poly(*t*BA) (blue, green, purple lines). All the spectra were overlapped.

about -123 to -124 ppm). The reduction in the signal intensity at -123 to -124 ppm suggests that the cleavage of C–F bond of $-\text{CF}_2-$ in TrFE unit initiated the graft polymerization of *t*BA. It has been also noted that these signals, originally doublets due to AB systems, are present as singlet upon grafting. This indicates that the AB system disappeared and became more simple system due to the introduction of flexible graft chains. From these findings, the grafting reaction occurs exclusively by abstracting a fluorine atom on the $-\text{CF}_2-$ of TrFE units, as shown in Scheme 2.

If ATRP of *t*BA was initiated by $-\text{CF}_2-$ groups of TrFE units, a fluorine atom must be attached to the propagating chain end of poly(*t*BA). However, it is still unclear whether the C–F bond continuously worked as a dormant species to generate the polymers by ATRP process or not, because the terminal halogen of the grafted poly(*t*BA) chains was very difficult to be identified by XPS and ATR-IR in this experiment. In general, homolytic cleavage of C–F bond hardly occurs due to large bonding energy compared with C–Cl and C–Br. One possible mechanism is that the halogen exchange of the fluorine to chloride would occur at the propagating chain end during ATRP in the presence of CuCl, because the C–Cl bonds has less bonding energy than the C–F ones.³⁰ The reversible oxidation and reduction cycles are possibly repeated between terminal C–Cl groups and CuCl/ligand complex catalysts due to the C–X bonds stability.

Surface-initiated ATRP of *t*BA and styrene from poly(VDF-*co*-TrFE) film surfaces

Surface-initiated ATRP of *t*BA or styrene from a poly(VDF-*co*-TrFE) films and successive hydrolysis or sulfonation were carried out as shown in Scheme 1. Poly(VDF-*co*-TrFE) copolymer does not dissolve in *t*BA nor styrene but slightly swells with the monomers, so that the polymerization initiates from the surface of the film and also partially from the bulk. XPS depth profiling using C_{60}^+ sputtering (Fig. S1 in ESI[†]) revealed gradient distribution of oxygen and fluorine atoms in-depth, indicating that outer most surface was almost covered with poly(*t*BA), while the mixture layer of poly(*t*BA) and poly(VDF-*co*-TrFE) was also formed inside the film. Thickness of surface-grafted poly(*t*BA) on poly(VDF-*co*-TrFE) film was estimated by sputter depth profiling to be 26.6

nm. Poly(*t*BA) was not found in deeper region (>83 nm) of the film. Therefore, the bulk poly(VDF-*co*-TrFE) chains remained inside the film. Details are described in ESI.[†] Unbound (free) polymers were also obtained simultaneously by sacrificial initiator, EC. Table 2 represents the reaction conditions of surface-initiated ATRP of *t*BA and styrene from poly(VDF-*co*-TrFE) films, and the M_n and molecular weight distribution (MWD) of the unbound polymers. The MWD values of the obtained poly(*t*BA) were $M_w/M_n = 1.3$ – 1.7 , which were rather broad, because 2-chloropropionate was used as a sacrificial initiator in this study, instead of 2-bromoisobutylate. In fact, it is known that the combination of 2-bromoisobutylate initiator and CuBr/PMDETA catalyst polymerizes *t*BA in a controlled manner to give the polymer with predictable M_n and narrow MWD.⁵³ However, the 2-bromoisobutylate initiates the polymerization of *t*BA much faster than poly(VDF-*co*-TrFE) thus yielding more free polymer, low-yield, and low- M_n surface-grafted polymer. Therefore, 2-chloropropionate and CuCl were used as a sacrificial initiator and catalyst, respectively, to regulate the polymerization rate in solution and to promote the simultaneous polymerization from free initiator and poly(VDF-*co*-TrFE) film, although the MWDs of free polymer become rather broad.

The film surface was analyzed by ATR-FTIR using a ZnSe ATR prism. ATR-FTIR spectra of the pristine, poly(*t*BA)-grafted, PAA-grafted and PAANA-grafted poly(VDF-*co*-TrFE) films are shown in Fig. 5. The characteristic absorption band appeared at 1723 cm^{-1} corresponding to the ester carbonyl group of poly(*t*BA). Absorption peaks corresponding to the C–H bond stretching vibrations (2934 cm^{-1} , 2979 cm^{-1} , 3008 cm^{-1}) considerably increased compared with the initial poly(VDF-*co*-TrFE) films.⁶ After hydrolysis reaction, the broadening of carbonyl stretching vibration to the lower wavenumber region and the absorption intensity decrease of C–H bond stretching vibration were observed indicating that the elimination of *tert*-butyl groups proceeded through the hydrolysis reaction. After neutralization, a new absorption corresponding to the carboxylic acid with counter cation was observed at 1575 cm^{-1} ,³⁶ indicating the formation of carboxylic acid sodium salt units.

ATR-FTIR spectra of the pristine, poly(VDF-*co*-TrFE)-*g*-poly(*t*BA) and poly(VDF-*co*-TrFE)-*g*-PS films are shown in Fig. 6. Aromatic C=C bond stretching vibrations (1493 cm^{-1} , 1601

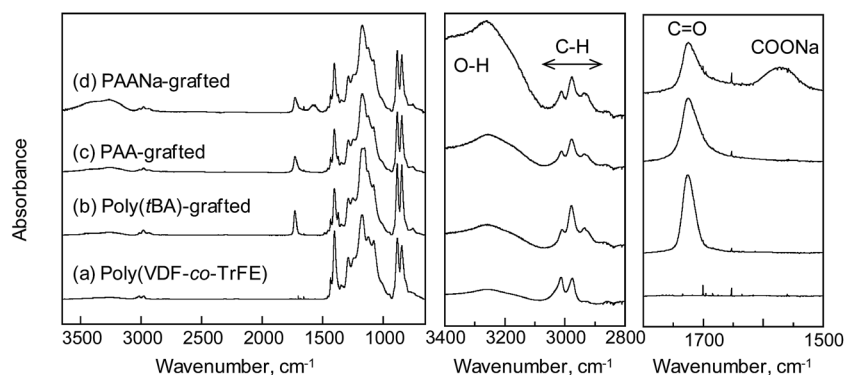


Fig. 5 ATR-IR spectra of (a) poly(VDF-*co*-TrFE) film, (b) poly(VDF-*co*-TrFE)-*g*-poly(*t*BA), (c) poly(VDF-*co*-TrFE)-*g*-PAA, and (d) poly(VDF-*co*-TrFE)-*g*-PAANA films. Full-range spectra (left), narrow range from 2800 to 3400 cm^{-1} (center), narrow range from 1500 to 1800 cm^{-1} (right).

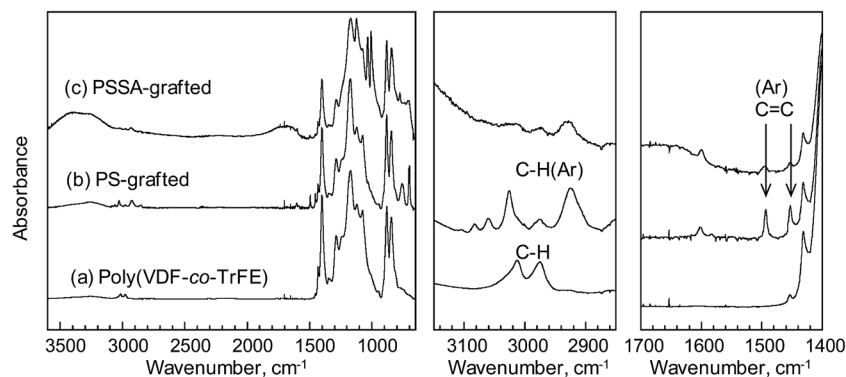


Fig. 6 ATR-FTIR spectra of (a) poly(VDF-*co*-TrFE) film, (b) poly(VDF-*co*-TrFE)-*g*-PS, and (c) poly(VDF-*co*-TrFE)-*g*-PSSA films. Full-range spectra (left), narrow range from 2850 to 3150 cm^{-1} (center), and narrow range from 1400 to 1700 cm^{-1} (right).

cm^{-1}) and aromatic C-H bond stretching vibrations (3025 cm^{-1} , 3060 cm^{-1} , 3082 cm^{-1}) are observed in the PS-grafted poly(VDF-*co*-TrFE) films. After the sulfonation reaction, a broad absorption attributable to the sulfonyl groups was clearly observed at 1620 cm^{-1} as well as the absorptions derived from aromatic rings, indicating the transformation of the aromatic rings to the styrene sulfonic groups.

The surface modified poly(VDF-*co*-TrFE) surfaces were also confirmed by XPS measurement as shown in Fig. 7. XPS spectra of the poly(VDF-*co*-TrFE)-*g*-poly(*t*BA) films exhibited a large decrease in fluorine peak intensity. Three peaks at 688, 532, and 285 eV were observed on the poly(VDF-*co*-TrFE)-*g*-poly(*t*BA) films, corresponding to fluorine, oxygen and carbon, respectively. The atomic ratios of C/O/F in the poly(VDF-*co*-TrFE)-*g*-poly(*t*BA) films were estimated to be 75.1/21.3/3.6, which is relatively close to the theoretical values calculated from the atomic assigned to poly(*t*BA) (C/O = 72.4/27.6) (Table 3). The narrow scan spectrum of C_{1s} showed peaks corresponding to the carbons of C=O, C-O, and C-C bonds, respectively (in Fig. S2, ESI[†]), due to poly(*t*BA). Although the C_{1s} peak of CF_2 bond was also slightly observed (3.2%) in narrow scan spectrum, the area ratio of three main peaks due to C=O, C-O, and C-C calculated by three fitting curves relatively agreed with poly(*t*BA). The intensity of C_{1s} peak due to the C-F bond (700 eV) was very low in Fig. 7, indicating that the poly(*t*BA) brush layer is thick enough to cover the poly(VDF-*co*-TrFE) film surface. After hydrolysis reaction, atomic ratio of C_{1s} considerably reduced and C/O/F ratio was calculated to be 66.7/11.5/21.8. The atomic ratios disagree with PAA and the fluorine content increased significantly, indicating the incomplete hydrolysis and the thickness reduction as well as the graft-density reduction through the elimination of bulky *tert*-butyl groups. The detachment of grafted poly(VDF-*co*-TrFE)-*g*-PAA chains on the hydrolysis reaction process is also expected. After neutralization, Na_{1s} peak was observed whereas the atomic ratio of Na was insufficient for complete neutralization calculated from O_{1s} based atomic ratio. The relatively high pK_a of the PAA would lead to the partial neutralization only.

XPS spectrum of the poly(VDF-*co*-TrFE)-*g*-PS films exhibited C_{1s} peaks with a large fluorine peak, indicating a low graft-density and low thickness. Three peaks at 180, 240, and 285

eV were observed on poly(VDF-*co*-TrFE)-*g*-PSSANa films, corresponding to S_{2p} , S_{2s} and O_{1s} , respectively. The atomic ratio of S/O in the poly(VDF-*co*-TrFE)-*g*-PSSA films were estimated to be approximately 1/3, indicating the formation of sulfonyl groups. After neutralization, Na_{1s} peak was observed, and the atomic

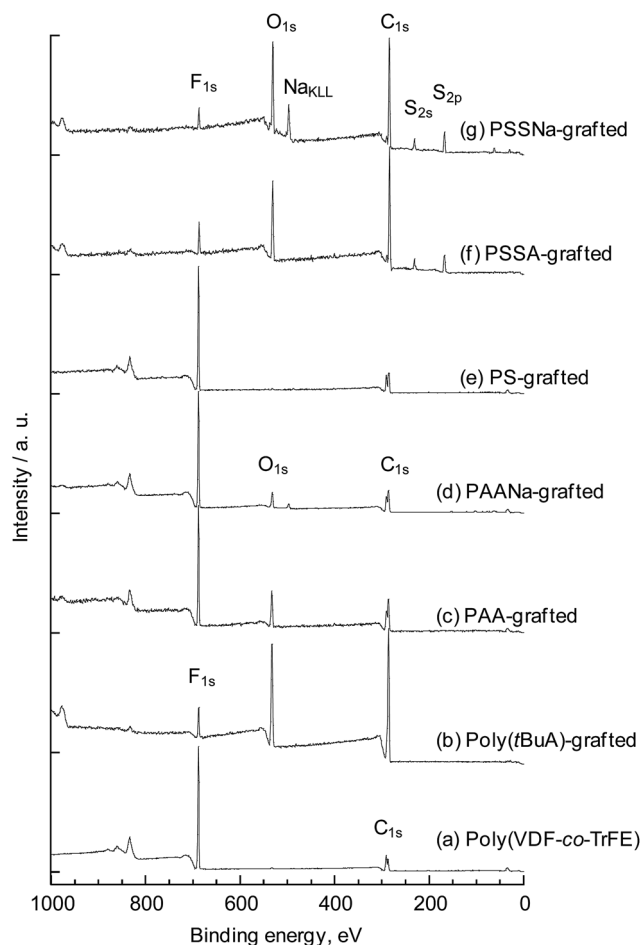


Fig. 7 XPS spectra of (a) poly(VDF-*co*-TrFE), (b) poly(VDF-*co*-TrFE)-*g*-poly(*t*BA), (c) poly(VDF-*co*-TrFE)-*g*-PAA (d) poly(VDF-*co*-TrFE)-*g*-PAANa, (e) poly(VDF-*co*-TrFE)-*g*-PS, (f) poly(VDF-*co*-TrFE)-*g*-PSSA, and (g) poly(VDF-*co*-TrFE)-*g*-PSSANa films.

Table 3 Atomic ratio of the poly(VDF-co-TrFE) film and surface modified poly(VDF-co-TrFE) film by surface-initiated polymerization^a

Sample	C _{1s}	O _{1s}	F _{1s}	S _{2p}	Na _{1s}
Poly(VDF-co-TrFE) copolymer	0.499	—	0.501	—	—
Poly(VDF-co-TrFE)-g-poly(<i>t</i> BA)	0.751	0.213	0.036	—	—
Poly(VDF-co-TrFE)-g-PAA	0.667	0.115	0.218	—	—
Poly(VDF-co-TrFE)-g-PAANa	0.559	0.080	0.347	—	0.014
Poly(VDF-co-TrFE)-g-PS	0.609	—	0.391	—	—
Poly(VDF-co-TrFE)-g-PSSA	0.705	0.185	0.045	0.065	—
Poly(VDF-co-TrFE)-g-PSSANa	0.642	0.206	0.040	0.052	0.060

^a Observed by XPS spectra. See also Fig. 7.

ratio of S/Na was approximately 1/1 indicating the quantitative neutralization (*i.e.*; transformation of the sulfonic acid into sulfonate groups).

Fig. 8 shows the surface morphology of the poly(VDF-co-TrFE) films before and after the surface grafting of poly(*t*BA) observed by AFM. Some pattern was observed on the surface of original poly(VDF-co-TrFE) film, however, no remarkable roughness was noted. After the surface grafting of poly(*t*BA) on the poly(VDF-co-TrFE) films, the root mean square (rms) of the surface roughness increased from 8.72 nm to 23.8 nm in a dry state in the $3 \times 3 \mu\text{m}^2$ scanning area. The poly(VDF-co-TrFE) films are slightly swollen with *t*BA to induce the film deformation, and the roughness would be enhanced by the poly(*t*BA)-grafting. Also, the poly(VDF-co-TrFE)-g-poly(*t*BA) component would slightly dissolve into *tert*-butyl acrylate during the polymerization process making the surface rough.

The polymer-grafting and the subsequent hydrophilization were also confirmed by water contact angle measurement. Typical photographs of water droplets on the surfaces are

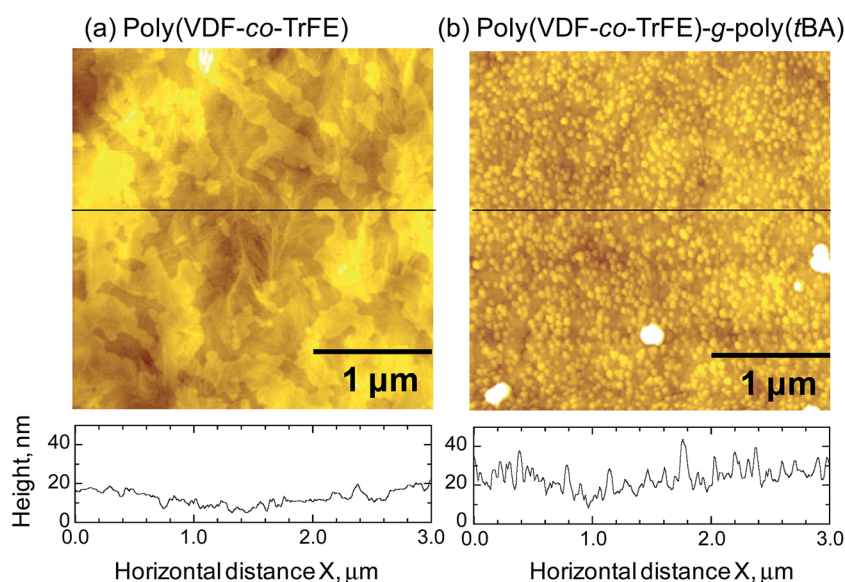


Fig. 8 AFM images ($3.0 \times 3.0 \mu\text{m}^2$) of the (a) poly(VDF-co-TrFE) film and (b) surface poly(VDF-co-TrFE)-g-poly(*t*BA) film. Vertical height profiles along with a line across the image are shown at the bottom of the top view images. The root mean square (rms) of the surface roughness of (a) and (b) were 8.72 and 23.8 nm in $3.0 \times 3.0 \mu\text{m}^2$ area, respectively.

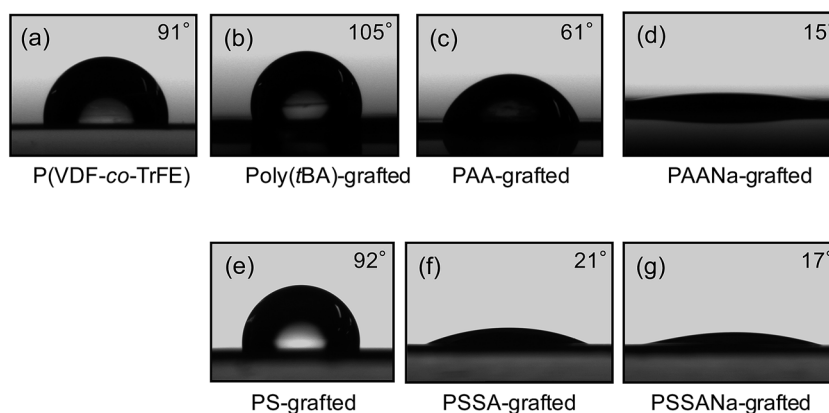


Fig. 9 Photographs (side view) of water droplets on (a) poly(VDF-co-TrFE), (b) poly(VDF-co-TrFE)-g-poly(*t*BA), (c) poly(VDF-co-TrFE)-g-PAA (d) poly(VDF-co-TrFE)-g-PAANa, (e) poly(VDF-co-TrFE)-g-PS, (f) poly(VDF-co-TrFE)-g-PSSA, and (g) poly(VDF-co-TrFE)-g-PSSANa films. Static water contact angles are represented inside of the images.

displayed in Fig. 9. The water contact angle on the pristine poly(VDF-co-TrFE) films was 91° , implying a slight hydrophobic behavior. Poly(*t*BA)-grafting increased the water contact angle to 105° , which is related to the low surface free energy of the *tert*-butyl groups. The *tert*-butyl groups segregate at the outermost surfaces due to the low surface free energy to afford a stable hydrophobic surface. The hydrolysis of the poly(VDF-co-TrFE)-*g*-poly(*t*BA) films and the sulfonation of poly(VDF-co-TrFE)-*g*-PS films drastically reduce the water contact angle. Especially, the styrene sulfonic acid groups make the water contact angle lower than those of graft polymer bearing carboxylic acid groups due to the large electrostatic interaction derived from the low pK_a .^{54–56} A water droplet on the neutralized polyelectrolyte brush surface of PAANa and PSSANa had further lower contact angles around 15–17 degree. The wettability and the surface free energy of neutralized polyelectrolyte brushes have been carefully investigated.⁵⁷ The electrostatic interaction makes the neutralized polyelectrolyte brush surface hydrophilic. Although the conversion of the hydrolysis, sulfonation and subsequent neutralization might not be complete, the hydrophilic chains segregate to the brush/water interface to show low contact angle similar to pure PAANa and PSAANa brushes. The hydrophilicity of PAANa-grafted and PSSANa-grafted films has been maintained for more than 3 months without any surface rearrangement by chain migration due to the thick modified layer unlike other hydrophilization techniques such as corona and γ -radiation treatments.

Conclusion

Direct modification of the poly(VDF-co-TrFE) films through surface-initiated ATRP of *t*BA and styrene, and the subsequent hydrophilization were demonstrated. The graft chains of poly(*t*BA) or PS were directly generated from the outermost surface of poly(VDF-co-TrFE) films by ATRP to afford a grafting layer with an approximately 10 nm thickness, although the graft density remains unclear. Subsequently, the acidic treatment of the surface-grafted film induced the hydrolysis of the *tert*-butyl ester or the sulfonation of the PS chains to yield a super hydrophilic and wettable surface on the hydrophobic poly(VDF-co-TrFE) films. ^1H and ^{19}F NMR analyses of the unbound (free) poly(VDF-co-TrFE)-*g*-poly(*t*BA), synthesized by direct ATRP of *t*BA onto poly(VDF-co-TrFE) copolymer in solution, revealed that the graft chains were covalently bonded with TrFE unit in the fluoropolymer backbone, suggesting that the homolytic cleavage of C–F bond of the $-\text{CF}_2-$ from TrFE units occurred in the presence of Cu catalyst to afford the radicals for the initiation reaction of the ATRP of vinyl monomers. This unique reactivity of TrFE made it possible to induce the direct “grafting-from” ATRP, thus enabling an effective and useful surface modification of the PVDF-based fluorine polymers.

Acknowledgements

The authors would like to thank all the companies that make this work possible.

References

- 1 B. Ameduri and B. Boutevin, *Well-Architected Fluoropolymers: Synthesis, Properties and Applications*, Elsevier, Amsterdam, 2004, pp.347–454.
- 2 B. Ameduri, *Chem. Rev.*, 2009, **109**, 6632–6686.
- 3 C. Brondino, B. Boutevin, J.-P. Parisi and J. Schrynemackers, *J. Appl. Polym. Sci.*, 1999, **72**, 611–620.
- 4 M. C. Clochard, J. Bégue, A. Lafon, D. Caldemaïson, C. Bittencourt, J. J. Pireaux and N. J. Betz, *Polymer*, 2004, **45**, 8683–8694.
- 5 J. J. Robin, *Adv. Polym. Sci.*, 2004, **167**, 235–247.
- 6 T. Soulestin, V. Ladmiraï, T. Lannuzel, F. Domingues Dos Santos and B. Ameduri, *Macromolecules*, 2015, **48**, 7861–7871.
- 7 V. S. D. Voet, G. ten Brinke and K. Loos, *J. Polym. Sci., Part A: Polym. Chem.*, 2014, **52**, 2861–2877.
- 8 E. T. Kang and Y. Zhang, *Adv. Mater.*, 2000, **12**, 1481–1494.
- 9 C. Wang and J. Chen, *Appl. Surf. Sci.*, 2007, **253**, 4599–4606.
- 10 Y. L. Liu, M. T. Luo and J. Y. Lai, *Macromol. Rapid Commun.*, 2007, **28**, 329–333.
- 11 F. Boschet and B. Ameduri, *Chem. Rev.*, 2014, **114**, 927–980.
- 12 H.-P. Brack, C. Padeste, M. Slaski, S. Alkan and H. H. Solak, *J. Am. Chem. Soc.*, 2004, **126**, 1004–1005.
- 13 G. H. Yang, Y. Zheng, K. S. Lee, E. T. Kang and K. G. Neoh, *J. Fluorine Chem.*, 2003, **119**, 151–160.
- 14 A. Okada, N. Ichinose and S. Kawanishi, *Polymer*, 1996, **37**, 2281–2283.
- 15 B. Soresi, E. Quartarone, P. Mustarelli, A. Magistris and G. Chiodelli, *Solid State Ionics*, 2004, **166**, 383.
- 16 L. Mascia, S. H. Pak and G. Caporiccio, *Eur. Polym. J.*, 1995, **31**, 459–465.
- 17 T. Liu, J. Y. Lee, E. T. Kang, P. Wang and K. L. Tan, *React. Funct. Polym.*, 2001, **47**, 201–213.
- 18 T. R. Dargaville, G. A. George, D. J. T. Hill and A. K. Whittaker, *Prog. Polym. Sci.*, 2003, **28**, 1355–1376.
- 19 M. C. Porte-Durrieu, C. Aymes-Chodur, N. Betz, B. Brouillaud, F. Rouais, A. LeMoel and C. Baquey, *Nucl. Instrum. Methods Phys. Res., Sect. B*, 1997, **131**, 364–371.
- 20 M. C. Porté Durrieu, C. Aymes Chodur, N. Betz and C. Baquey, *J. Biomed. Mater. Res.*, 2000, **52**, 119–127.
- 21 S. Holmberg, T. Lehtinen, J. Näsman, D. Ostrovskii, M. Paronen, R. Serimaa, F. Sundholm, G. Sundholm, G. Torell and M. Torkkeli, *J. Mater. Chem.*, 1996, **6**, 1309–1312.
- 22 M. Muller and C. Oehr, *Surf. Coat. Technol.*, 1999, **116–119**, 802–821.
- 23 J. Ennari, S. Hietala, M. Paronen, F. Sundholm, N. Walsby, M. Karjalainen, R. Serimaa, T. Lehtinen and G. Sundholm, *Macromol. Symp.*, 1999, **146**, 41–45.
- 24 S. Kaur, Z. Ma, R. Gopal, G. Singh, S. Ramakrishna and T. Matsuura, *Langmuir*, 2007, **23**, 13085–13092.
- 25 E. Katoh, C. Kawashima and I. Ando, *Polym. J.*, 1995, **27**, 645–650.
- 26 S. Holmberg, P. Holmlund, R. Nicolas, C. E. Wilén, T. Kallio, G. Sundholm and F. Sundholm, *Macromolecules*, 2004, **37**, 9909–9915.

- 27 A. Akthakul, A. I. Hochbaum, F. Stellacci and A. M. Mayes, *Adv. Mater.*, 2005, **17**, 532–535.
- 28 L. Sauguet, C. Boyer, B. Ameduri and B. Boutevin, *Macromolecules*, 2006, **39**, 9087–9101.
- 29 Y. W. Kim, D. K. Lee, K. J. Lee and J. H. Kim, *Eur. Polym. J.*, 2008, **44**, 932–939.
- 30 S. Samanta, D. P. Chatterjee, S. Manna, A. Mandal, A. Garai and A. K. Nandi, *Macromolecules*, 2009, **42**, 3112–3120.
- 31 S. Samanta, D. P. Chatterjee, R. K. Layek and A. K. Nandi, *Macromol. Chem. Phys.*, 2010, **212**, 134–149.
- 32 Y. Chen, D. Liu, Q. Deng, X. He and X. Wang, *J. Polym. Sci., Part A: Polym. Chem.*, 2006, **44**, 3434–3443.
- 33 Y. W. Kim, J. K. Choi, J. T. Park and J. H. Kim, *J. Membr. Sci.*, 2008, **313**, 315–322.
- 34 E. M. W. Tsang, Z. Zhang, Z. Shi, T. Soboleva and S. Holdcroft, *J. Am. Chem. Soc.*, 2007, **129**, 15106–15107.
- 35 Y. Chen, L. Ying, W. Yu, E. T. Kang and K. G. Neoh, *Macromolecules*, 2003, **36**, 9451–9457.
- 36 L. Ying, W. H. Yu, E. T. Kang and K. G. Neoh, *Langmuir*, 2004, **20**, 6032–6040.
- 37 Y. Chen, W. Sun, Q. Deng and L. Chen, *J. Polym. Sci., Part A: Polym. Chem.*, 2006, **44**, 3071–3082.
- 38 Z. Zhang, E. Chalkova, M. Fedkin, C. Wang, S. N. Lvov, S. Komarneni and T. C. M. Chung, *Macromolecules*, 2008, **41**, 9130–9139.
- 39 L. Yang, X. Li, E. Allahyarov, P. L. Taylor, Q. M. Zhang and L. Zhu, *Polymer*, 2013, **54**, 1709–1728.
- 40 L. Yang, E. Allahyarov, F. Guan and L. Zhu, *Macromolecules*, 2013, **46**, 9698–9711.
- 41 X. Hu, J. Li, H. Li and Z. Zhang, *J. Polym. Sci., Part A: Polym. Chem.*, 2013, **51**, 4378–4388.
- 42 J. F. Hester, P. Banerjee, Y. Y. Won, A. Akthakul, M. H. Acar and A. M. Mayes, *Macromolecules*, 2002, **35**, 7652–7661.
- 43 S. Inceoglu, S. C. Olugebefola, M. H. Acar and A. M. Mayes, *Des. Monomers Polym.*, 2004, **7**, 181–195.
- 44 E. M. W. Tsang, Z. Zhang, A. C. C. Yang, Z. Shi, T. J. Peckham, R. Narimani, B. J. Frisken and S. Holdcroft, *Macromolecules*, 2009, **42**, 9467–9480.
- 45 D. Valade, F. Boschet and B. Ameduri, *J. Polym. Sci., Part A: Polym. Chem.*, 2010, **48**, 5801–5811.
- 46 K. Ishihara, Y. Iwasaki, S. Ebihara, Y. Shindo and N. Nakabayashi, *Colloids Surf., B*, 2000, **18**, 325–335.
- 47 A. E. Oezcam, K. E. Roskov, R. J. Spontak and J. Genzer, *J. Mater. Chem.*, 2012, **22**, 5855–5864.
- 48 M. Kobayashi, T. Matsugi, J. Saito, J. Imuta, N. Kashiwa and A. Takahara, *Polym. Chem.*, 2013, **4**, 731–739.
- 49 T. Kimura, M. Kobayashi, M. Morita and A. Takahara, *Chem. Lett.*, 2009, **38**, 446–447.
- 50 S. Holmberg, P. Holmlund, C.-E. Wilén, T. Kallio, G. Sundholm and F. Sundholm, *J. Polym. Sci., Part A: Polym. Chem.*, 2002, **40**, 591–600.
- 51 M. Zhang and T. P. Russell, *Macromolecules*, 2006, **39**, 3531–3539.
- 52 J. K. Koh, Y. W. Kim, J. T. Park and J. H. Kim, *J. Polym. Sci., Part B: Polym. Phys.*, 2008, **46**, 702–709.
- 53 K. A. Davis and K. Matyjaszewski, *Macromolecules*, 2000, **33**, 4039–4047.
- 54 Z. Mao, L. Ma, C. Gao and J. Shen, *J. Controlled Release*, 2005, **104**, 193–202.
- 55 R. D. Porasso, J. C. Benegas and M. A. G. T. van den Hoop, *J. Phys. Chem. B*, 1999, **103**, 2361–2365.
- 56 S. Holmes-Farley, R. H. Reamey, T. J. McCarthy, J. Deutch and G. M. Whitesides, *Langmuir*, 1985, **1**, 735–740.
- 57 M. Kobayashi, Y. Terayama, H. Yamaguchi, M. Terada, D. Murakami, K. Ishihara and A. Takahara, *Langmuir*, 2012, **28**, 7212–7222.